DEPTH PERCEPTION FROM MOTION UNDER VIEWPOINT DISTORTION

BUI NHAT LINH

(*B. Eng. Hanoi University of Technology*)

A THESIS SUBMITTED

FOR THE DEGREE OF MASTER OF ENGINEERING

DEPARTMENT OF ELECTRICAL AND COMPUTER ENGINEERING

NATIONAL UNIVERSITY OF SINGAPORE

2008

Acknowledgments

It gives me great delight to acknowledge the following people who have helped me to finish this project:

My deepest thanks go to my supervisor, Dr. Cheong Loong Fah, for his constant support, encouragement, and patience throughout the years. I would like to thank Dr. Valerie Cornilleau-Pèrés, Dr. Yen Shih-Cheng, Dr. Chua Fook Kee for helpful psychophysical discussions and comments.

I am grateful to our laboratory technician Mr. Francis Hoon for providing me with technical facilities.

I also wish to thank the following experimental candidates.

- Nguyen Tan Dat
- Pham Duc Chuyen
- Li Shimiao
- Hew Litteen
- Loke Yuan Ren

Lastly, I would also like to thank to all others who have contributed to this project.

Contents

Summary

We investigated the monocular perception of slant and tilt under viewpoint distortion when the only depth cue was motion parallax. Viewpoint distortion is the distortion due to the difference between the projection point of the projector system and the viewpoint of the subjects. Our computational modeling showed that viewpoint distortion could be regarded as an equivalent distortion in the intrinsic camera parameters.

Psychophysical experiments were designed to examine how human subjects perceived depth when viewpoint distortion occurred. A plane containing random dots rotating-in-depth was displayed to subjects who would then use a probe to indicate the perceived orientation of the plane. The viewpoint distance and the projection point were changed to produce viewpoint distortion. The tilt and slant of the perceived plane were analyzed to evaluate the effect of viewpoint distortion on depth perception. In the first experiment, slant perception under viewpoint distortion was examined. The second experiment was designed, in particular, to investigated slant perception under viewpoint distortion in large field of view. We studied tilt perception in the third experiment.

Our experimental results suggested that human perception was not affected significantly under viewpoint distortion. The data analysis cannot find any effect of viewpoint distortion on tilt perception. Only a weak effect of viewpoint distortion on slant perception was observed in the case of large slant magnitudes.

A computational explanation of the viewpoint distortion was provided. We first proved that the viewpoint distortion in our psychophysical experiments was equivalent to a change in the focal length. Using the optical flow equations and the iso-distortion framework, we could prove that a change in the focal length did not affect significantly tilt and slant perception.

List of Figures

List of Tables

Chapter 1

Introduction

The human perception of $3D$ space partly arises from motion field. It has been shown that motion parallax is a critical cue in the perception of depth [45], and in the detection of surface curvature [11]. As a consequence, structure from motion has become one of the central topics of the computer vision community and has received constant attention since the 1980s [21, 22, 23, 27]. With the recent development of various Virtual Reality application, the question that arises is how people perceived depth from viewing a moving sequence of image through a Head Mounted Display (HMD), e.g. flight simulation for training pilot.

Perception from moving sequence of image is distorted by the difference between the camera projection point and the viewpoint. The projection point is the position where the camera center is; the viewpoint is the position of the observer's eyes. Theoretically, only the observer located exactly at the projection point sees the right version of the pictures. When the viewpoint is not identical with the projection point, observer will receive visual stimuli including dynamic cues such as optical flow different from

the moving sequence of image. As a result, depth perception from motion cues will be affected. This distortion from the difference between the projection point and the viewpoint will be called viewpoint distortion. Henceforth our experiments are designed to examine how depth perception from motion changed because of this viewpoint distortion.

The viewpoint distortion has been studied by a few researchers in last three decades. Hagen [19] examined if people could recognize relative size of images in different viewing position. The stimuli was photographs of triangle and square images against a textured background. Experimental results showed that the viewpoint did not affect much the percentage of correct choices. Rosinski et al [34] carried out experiments about the perception of picture surface. The viewing was monocular through an aperture. It was found out that the dependence of judged slant on the projection slant for different viewpoints was very similar. Perkins [44] explained that observer's expectation of known shapes compensated for the distortion arising from viewpoint change. The observer seemed to forced the percept of objects to a familiar shapes (cube, circle) or following some rules (parallel, orthogonal of line).

All the proceeding works only dealt with static object. With the development of the digital age, moving sequence of image became popular in many applications. Moving sequence of image give the spectators the feel of reality with the changing of objects in time and in space. Usually perception from motion cues is critical. In flight simulation, the screen duplicated the view of a pilot from the sky. The depth information is the most important information in flight simulation. It decides how far from the plane to the target or to the landing site. In this case, with very far distances, all depth cues except the depth from motion cue are inactive. In Virtual Reality application with

HMD, the 3D effect mainly comes from the moving images that changing according to the movement and the orientation of the subjects. Again, depth from motion is the primary source. Thus perception from motion, especially depth from motion, should be the principal object of research in human perception from picture.

In this work, we focus on how plane orientation in $3D$ space is recovered from moving images. The visual perception of plane orientation is necessary when climbing a slope or in various action like grasping [51]. Stevens [46] described the plane orientation by tilt and slant. We denoted N as the vector normal to a plane. The tilt τ is the angle the projection of N onto the image plane makes with the positive x-axis (the direction of N_f). The slant σ is the angle between N and the Z-axis. Tilt computation requires only ordinal relationship between object points [29], but absolute metrical depth is necessary to recover slant.

Computational studies showed that plane orientation could be computed from motion [31]. These approaches described the optical flow of a moving plane as a second-order polynomial of image coordinates.They indicated however that there exists ambiguity in the problem of solving the plane equation from optical flow. In general, there are two solutions. It made the well-known **N-T** ambiguity between the plane orientation and the frontal translation.

In visual psychophysics, plane orientation recovered from motion has been intensively researched. It is well-known that perception of slant is distorted and not reliable. In an experiment of planes rotating in depth under orthographic projection, Domini and Caudek [16] reported that perceived slant was not significantly influenced by the simulated slant. Instead, slant was influenced by tilt and increased with the tilt. In

similar set-up, Todd and Perotti [49] showed that slant depends both on tilt and on deformation $def = \sqrt{u_x^2 + u_y^2}$. In contrast, both Domini and Caudek [16],Todd and Perotti [49] reported that tilt estimation was more accurate than slant. For details of the tilt perception from motion, Zhong et al [51] studied the dependence of tilt estimation on field of view (FOV) and on the angle between the tilt and the frontal translation (translation projected onto the image plane).

In all the above psychophysics experiments, viewpoint distortion has not been studied. Under orthographic projection, the point of projection is irrelevant as the observer received the same images in from different distances. Under perspective projection, the stimuli was always projected with the centre of perspective projection located at the subject's eyes. Until now, the effect of the viewpoint distortion on plane perception from motion is still an open question. In our computational studies, the viewpoint distortion is equivalent to an error of intrinsic parameters. We carries out psychophysics experiments to test our theory. Our experiments are designed to examine the distortion of perceived plane orientation from motion cues under distorted viewpoint conditions. In fact, the distorted condition in our experiments is the difference between the distance from viewpoint and project point to the screen.

We first introduce the theory behind the computation of tilt and slant from optic flow(Chapter 2). We then follow up by describe iso-distortion framework [6], which will be used to explain the result of the experiments. In the next three Chapter 3,4, and 5, psychophysical experiments are documented. In our experiments, a plane containing random dots rotating in depth was displayed to subjects who would then use a probe to indicate the perceived direction of plane. The viewpoint distances and the projection distances are changed. Tilt and slant of the perceived plane were analyzed to evaluate

the effect of viewpoint distortion to depth perception. Slant is studied in Experiment 1 (Chapter 3). Experiment 2 is designed to study slant perception in large FOV. In Experiment 3 (Chapter 4), tilt perception is examined. Our experimental results show that human subject can adapt well to the viewpoint distortion. In chapter 5, we first introduce our computational modeling for viewpoint distortion. We prove that the viewpoint distortion in our psychophysical experiments could be regarded as a change in focal length. Applying optical flow equations and iso-distortion framework, we then explain how human visual system manifests the kind of performance we witnessed in the experiments under viewpoint distortion.

Chapter 2

Background

2.1 Introduction

The objective of our research program is to bring about new understanding of how a visual system derives depth information from motion cues. Our approach is through a cross-breeding of methodology in the fields of computational vision and visual psychophysics. On the one hand, we develop computational models that appropriately account for the psychophysical phenomena. On the other hand, we conduct psychophysical experiments to support the theories proposed in the computational studies, and in turn gain new ideas from human vision to apply to computer vision. In this chapter, we review some background in both computational vision and visual psychophysics that are related to our work. This review also includes some of the more recent research findings reported by members of our project team.

2.2 Computational studies

2.2.1 Optical flow

Optical flow is "a vector field subject to the constraint in equation (2.1) and loosely defined as a apparent motion of the image brightness motion"

$$(\nabla E)^T v + E_t = 0 \tag{2.1}$$

where $E = E(x, y, t)$ is the image brightness and v is the motion field, E_t is the partial derivative of E with respect to time. This is the well known optical flow equation. Let n denote a unit vector along (E_x, E_y) then the optical flow equation can be written as:

$$(v_x, v_y)(n_x, n_y) = v_n = -\frac{E_t}{\|\nabla E\|} \tag{2.2}$$

V_n at any point can also be thought of as the image velocity component normal to the iso-intensity contour through that point. Therefore, the optical flow equation implies that at any point only that component of image velocity normal to the iso-intensity through that point can be determined. Some heuristic assumptions have been introduced to measure both components of the optical flow. Three common approaches are:

- Impose smoothness constraint on flow.

- Assume velocity is locally constant.

- Assume local parametric model.

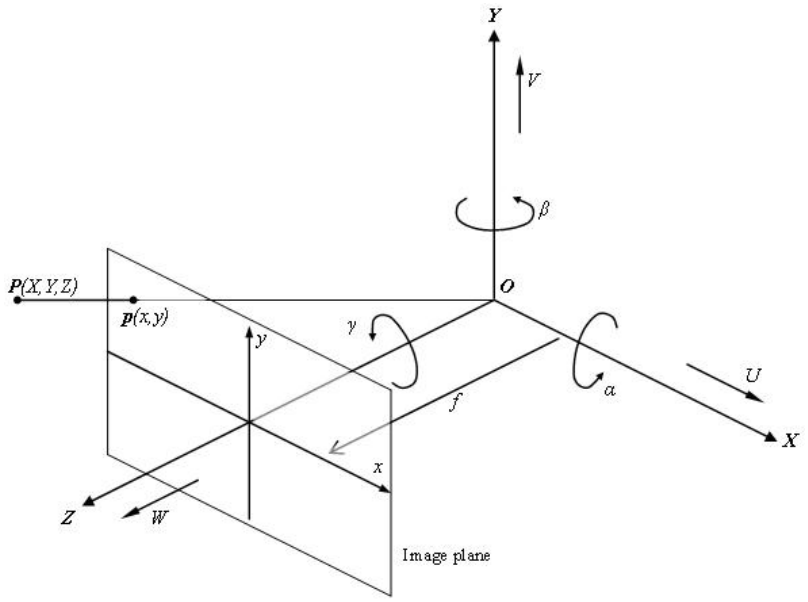

Figure 2.1: Space and object model showing global and image coordinate system

2.2.2 3D Space model

Figure 2.2.2 describes the imaging model used: The origin O is at the optic center of the observer's eye (or the focal point of the camera). A point in space is defined by its coordinates (X, Y, Z) with respect to this origin. The positive Z-axis is the direction of the optical axis of the viewing system and the image plane is modeled as a flat plane parallel to the XY-plane, a distance of focal length f from the origin. The relative motion between the observer and object can be decomposed into a translation component $\mathbf{T} = (U, V, W)$ and a rotation component $\mathbf{R} = (\alpha, \beta, \gamma)$. Vector $T_f(U, V)$ is called frontal translation. The object is said to be rotating in depth if α and/or β is non-zero.

A point $\mathbf{P}(X,Y,Z)$ has an image $\mathbf{p}(x,y)$ on the image plane, which can be obtained

using the perspective projection rules:

$$x = \frac{fX}{Z} \tag{2.3}$$

$$y = \frac{fY}{Z} \tag{2.4}$$

2.2.3 Plane equation

The general equation of a plane is given by

$$Z = Z_X X + Z_Y Y + Z_O \tag{2.5}$$

where Z_X and Z_Y are the derivatives with respect to the X-axis and Y-axis, and Z_O is the intercept of the plane with the line of sight. In this report, Z_O may sometimes be referred to as the distance of the plane from the observer. Under perspective projection, there is an alternative form of plane equation using the image coordinates:

$$p = p_x x + p_y y + p_0 \tag{2.6}$$

where $p = \frac{1}{Z}$, $p_x = \frac{-Z_X}{Z_0}$, $p_y = \frac{-Z_Y}{Z_0}$, and $p_0 = \frac{1}{Z_0}$

The plane normal is given by $N = (p_x, p_y, p_0)$. The vector $N_f = (p_x, p_y)$ is the projection of N onto the frontal-parallel plane.

The orientation of the plane can be described by the tilt τ and slant σ. Tilt is the angle between N_f and positive x-axis. Slant is the angle between N and the Z-axis.

$$\tau = \tan^{-1} \frac{p_y}{p_x} \tag{2.7}$$

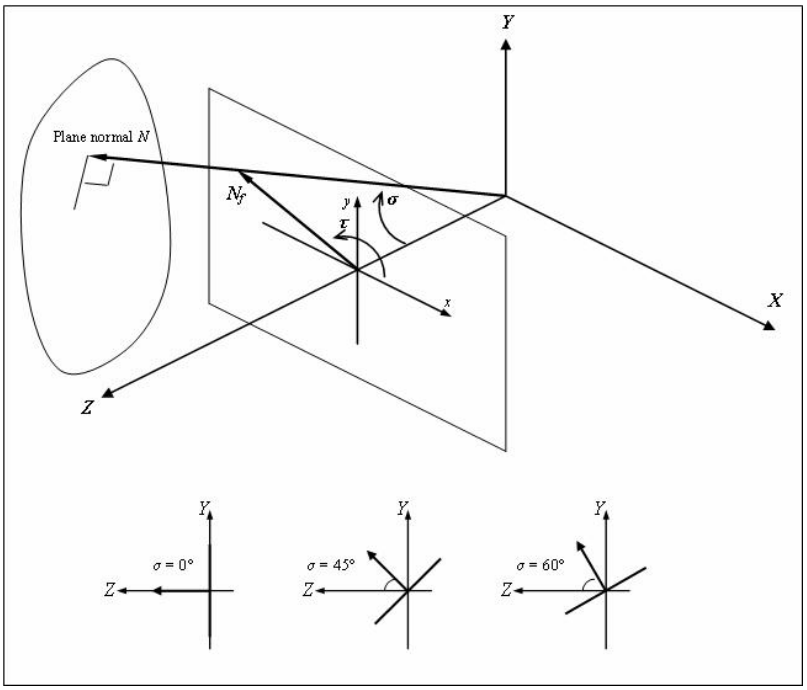

Figure 2.2: The tilt and slant of a plane

$$\sigma = \tan^{-1} \sqrt{\frac{p_x^2 + p_y^2}{p_0^2}} \tag{2.8}$$

In this report, we use the term winding angle [14] to describe the angle between T_f and N_f.

2.2.4 Projection model

In the following, we assume that the focal length $f = 1$

Perspective projection

$$x = \frac{X}{Z} \tag{2.9}$$

$$y = \frac{Y}{Z} \tag{2.10}$$

For an observer translating with $T = (U, V, W)$ and rotating with $R = (\alpha, \beta, \gamma)$ about the origin O, the instantaneous velocity of the point $P(X, Y, Z)$ is:

$$\dot{X} = -U - \beta Z + \gamma Y \tag{2.11}$$

$$\dot{Y} = -V - \gamma X + \alpha Z \tag{2.12}$$

$$\dot{Z} = -W - \alpha Y + \beta X \tag{2.13}$$

If P is a point on the plane, the velocity of its image $p(x, y)$ is:

$$u = \dot{x} = u_0 + u_x x + u_y y + u_{xx} x^2 + u_{xy} xy \tag{2.14}$$

$$v = \dot{y} = v_0 + v_x x + v_y y + v_{yy} y^2 + v_{xy} xy \tag{2.15}$$

where

$$u_0 = -(U p_0 + \beta) \tag{2.16}$$

$$u_x = -(U p_x - W p_0) \tag{2.17}$$

$$u_y = -(U p_0 - \gamma) \tag{2.18}$$

$$u_{xx} = W p_x - \beta \tag{2.19}$$

$$u_{xy} = W p_y + \alpha \tag{2.20}$$

$$v_0 = -(V p_0 - \alpha) \tag{2.21}$$

$$v_x = -(V p_x + \gamma) \tag{2.22}$$

$$v_y = -(Vp_y - Wp_0) \tag{2.23}$$

$$v_{yy} = Wp_y + \alpha \tag{2.24}$$

$$v_{xy} = Wp_x - \beta \tag{2.25}$$

$$\tag{2.26}$$

Orthographic Projection

This model does not bring any perspective information into the image. It is often used to approximate perception in small field.

$$x = X \tag{2.27}$$

$$y = Y \tag{2.28}$$

Under orthographic projection, the optic flow contains only first-order terms:

$$u = \dot{x} = u_0 + u_x x + u_y y \tag{2.29}$$

$$v = \dot{y} = v_0 + v_x x + v_y y \tag{2.30}$$

where:

$$u_0 = -(U + \beta Z_0) \tag{2.31}$$

$$u_x = -\beta Z_x \tag{2.32}$$

$$u_y = -(\beta Z_y - \gamma) \tag{2.33}$$

$$v_0 = -(V - \alpha Z_0) \tag{2.34}$$

$$v_x = -(\gamma - \alpha Z_x) \tag{2.35}$$

$$v_y = -\alpha Z_y \tag{2.36}$$

From the optic flow equations above, if $u_0 = v_0 = \gamma = 0$(as in the case of a rotation about a fronto-parallel axis through the centre of the plane), we are unable to extract an expression for the slant, and there are generally two solutions for the tilt direction.

2.2.5 N-T Ambiguity

Longuet-Higgins ([32]) showed that, under the case of perspective projection, in general there is a twofold ambiguity when solving this set of non-linear equations (2.17)-(2.26), with the roles of the vectors N (the plane normal) and T being interchangeable. The exceptions are

1. when the translation along the line of sight is zero (i.e. $W = 0$), in which case a unique solution is obtained from the reduced set of linear flow equations,

2. when the translation is parallel to the surface normal, in which case the two solutions coincide.

In the presence of the twofold ambiguity, the relation between the dual solutions is:

$$T' = Z_0 W N \tag{2.37}$$

$$N' = \frac{T}{Z_0 W} \tag{2.38}$$

$$R' = R - Z_0(T \times N) \tag{2.39}$$

In other words, the directions of N and T are interchanged.

2.2.6 Tilt and slant in lateral motion

In this report, we use the term lateral motion to describe the motion comprising a rotation $R = (0, \beta, 0)$ and a translation $T = (U, 0, W)$ where $U >> W$. Lateral motion is prevalently used in psychophysical experiments involving motion cues and is known to produce a better depth information from motion cues [9].

Under such motion, the set of optic flow components are reduced to

$$u_0 = -(Up_0 + \beta) = 0 \tag{2.40}$$

$$u_x = = -(Up_x - Wp_0) \tag{2.41}$$

$$u_y = -Up_y \tag{2.42}$$

$$u_{xx} = Wp_x - \beta \tag{2.43}$$

$$u_{xy} = Wp_y \tag{2.44}$$

$$v_0 = 0 \tag{2.45}$$

$$v_x = 0 \tag{2.46}$$

$$v_y = Wp_0 \tag{2.47}$$

$$v_{yy} = Wp_y \tag{2.48}$$

$$v_{xy} = Wp_x - \beta \tag{2.49}$$

In this case, tilt can be recovered from the first order components of optical flow. However the second order components are necessary for the recovery of slant:

$$\tau = \tan^{-1} \frac{u_y}{u_x - v_y} \tag{2.50}$$

$$\sigma = \tan^{-1} \sqrt{\frac{u_{xy}^2(u_y^2 + (u_x - v_y)^2)}{u_y^2 v_y^2}} \tag{2.51}$$

In this case, the spurious solution arising from the $N - T$ ambiguity, given by $T' = Z_0 W(p_x, p_y, p_o)$ and $N' = (U, 0, W)/Z_O W$, is not a realistic choice for the observer. This is because in our case of lateral motion where $U \gg W$, the ambiguity solution would represent an extremely slanted plane with its normal almost lying in the fronto-parallel plane. This percept is not compatible with the stimulus covering a large part of the visual field. In the extremely case where W=0, in fact a unique solution is obtained.

2.2.7 Error in focal length

In structure from motion, it is common to assume that the camera is calibrated and the focal length is fixed. However, with the advent of zoom lenses, the focal length of a camera is often not fixed. Changes can come from zooming or because of the viewing environment such as wearing a HMD. In many cases, it is not possible to stop the camera to recalibrate. During calibration, the camera is forced to do a special motion or view a special calibration object. Even with these constraints, there are some ill-conditioned cases that can result in ambiguous solutions.

There are a few works about the effect of errors in focal length on depth reconstruction. Recently, Cheong and Peh ([8]) studied the distortion in reconstruction from 3D motion with varying focal length. In the case where the focal length is unknown, depth relief can still be obtained. In addition, Cheong and Xiang ([9])demonstrated how erroneous focal length affects the bas-relief ambiguity.

2.3 Iso-distortion framework

The iso-distortion framework was first introduced by Cheong et al. [6]. The isodistortion framework seeks to understand the distortion due to some errors in the estimated camera parameters. 3-D motion estimation is regarded as the first step towards the full recovery of 3-D shape information from 2-D measurements. Therefore any error in the 3-D motion estimates will systematically affect the perceived space. However, the reliability of depth estimates could have quite a different behavior from that of 3-D motion estimates. That is, motion-scene configuration that allows robust motion recovery may yield less than desirable depth estimates, and vice versa. Another substantive question is of course, whether there is any interaction between errors in motion estimates and the corresponding distortion in the recovered depth. That is, would the distortion in the perceived space in turn affect motion estimation? Partially to address these questions, the iso-distortion framework was introduced in [6]. The iso-distortion framework seeks to understand the geometric laws under which the recovered scene is distorted due to some errors in estimated motion parameters. The distortion in the perceived space is visualized by looking at the locus of constant distortion, known as the iso-distortion surfaces. The iso-distortion framework is employed by us to analyze the behavior of depth estimation. In this section, we revisit some notations that would be useful for this thesis.

The scaled depth of a scene point recovered can be written as

$$Z = \frac{(x - x_0, y - y_0) \cdot \mathbf{n}}{(u - u_{rot}, v - v_{rot}) \cdot \mathbf{n}} \tag{2.52}$$

where $\mathbf{n}$ is an unit vector in the image plane which specifies a direction.

If there are some errors in the estimation of extrinsic parameters, this will in turn cause errors in the estimation of scaled depth, and thus a distorted version of the space will be computed. The estimated depth $\hat{Z}$ can be readily shown to be related to the actual depth Z as follows:

$$\hat{Z} = Z\left(\frac{(x-\hat{x}_0, y-\hat{y}_0)\cdot\mathbf{n}}{(x-x_0, y-y_0)\cdot\mathbf{n} + Z\left(u_{rot_e}, v_{rot_e}\right)\cdot\mathbf{n} + Z(u_n, v_n)\cdot\mathbf{n}}\right) \tag{2.53}$$

where (u_n, v_n) is a noise term representing error in the estimate for the optical flow, the "ˆ" symbol represents the estimated quantity, those terms with the subscript "e" represent the errors in those quantities.

From (2.53) we can see that $\hat{Z}$ is obtained from Z through multiplication by a factor given by the terms inside the bracket, which we denote by D and call the distortion factor. The expression for D contains the term $\mathbf{n}$ whose value depends on the scheme we use to recover depth. In the optical-flow based approach, however, a possible scheme is to recover depth along the estimated epipolar direction, based on the intuition that the epipolar direction contains the strongest translational flow. It means that we first project optical flow along the direction emanating from the estimated FOE and then recover depth along that direction, i.e. $\mathbf{n} = \frac{(x-\hat{x_0}, y-\hat{y_0})^T}{\sqrt{(x-\hat{x_0})^2+(y-\hat{y_0})^2}}$, or in the case of $\hat{W} = 0$ where the estimated FOE is at infinity, $\mathbf{n} = -\frac{(\hat{U},\hat{V})^T}{\sqrt{\hat{U}^2+\hat{V}^2}}$. Upon substituting the corresponding value of $\mathbf{n}$ for the case of epipolar reconstruction approach, we obtain the following expression for the distortion factor:

$$D = \frac{(x-\hat{x}_0)^2 + (y-\hat{y}_0)^2}{(x-x_0, y-y_0)\cdot(x-\hat{x}_0, y-\hat{y}_0) + Z\left(u_{rot_e}+u_n, v_{rot_e}+v_n\right)\cdot(x-\hat{x}_0, y-\hat{y}_0)} \tag{2.54}$$

Ignoring the noise term for the moment, we see that for specific values of the parameters x_0, y_0, $\hat{x}_0$, $\hat{y}_0$, α_e, β_e, γ_e and $\mathbf{n}$, and for any fixed distortion factor D, equation (2.53) describes a surface $g(x, y, Z) = 0$ in the xyZ-space, which is the iso-distortion surface. This iso-distortion surface has the obvious property that points lying on it are distorted in depth by the same multiplicative factor D. The systematic nature of the distortion can then be made clear by looking at the organization of these iso-distortion surfaces. Sometimes to facilitate the pictorial description of these surfaces, we slice them with planes parallel to either the xZ-plane or the xy-plane. We call the curves thus obtained on the planar slice the iso-distortion contours.

2.3.1 Distortion under lateral and forward motion

In an attempt to further develop the iso-distortion framework, Cheong and Xiang ([9]) investigate the characteristics of depth distortion experienced under two kinds of motion: lateral and forward translations. They argue that the two motions are not equal in terms of robust depth recovery and there exists certain dichotomy between forward and lateral translations. It is thus important to adopt a good motion strategy so as to obtain reliable depth information.

In the descriptions of their work, Cheong and Xiang ([9]) make several assumptions. First, they assume that the agent executing the motion is at least aware that such generic type of motion is being executed. That is, when the agent is making lateral motion, it is aware that no forward motion is made. Similarly, when it is making a forward motion, it is aware that no lateral motion is executed. This assumption seems reasonable since the motion is likely to be purposely executed for depth recovery by

the agent. Second, they assume that the field of view is small so that second order effect can be neglected. Third, the error contributed by rotation about the optical axis is assumed to be negligible.

With the above assumptions, they find that when lateral translation was executed, the distortion factor could be very much simplified. The distortion transformation reduces to an invertible projective transformation with most of the elements in the matrix representing the transformation being zero. In fact, it has the effect of generating a relief transformation that possesses some nice properties. Under certain conditions that can be satisfied easily, the ordinal depth information can be obtainable. Moreover, if the errors caused by the rotation are totally eliminated (i.e. error is only in the lateral translation), all of the first order and second order shapes can be preserved. However, with a large field of view or if the contribution of error in rotation about the optical axis is not negligible, the global ordinal depth information may not be obtainable. The preservation of ordinal depth is only restricted to a localized region. The size of this localized region is dependent on the size of the motion errors, the respective image coordinates and the depth difference.

2.3.2 Distortion under calibration uncertainty

Cheong and Xiang ([9]) further extend their work to account for the effects of calibration uncertainty on the depth recovery under the two simple motion types. In other words, the motion errors are not restricted to the extrinsic parameters. The intrinsic parameters of the camera are allowed to vary over time (e.g. in zooming). They conclude that with varying intrinsic parameters, depth relief can only be preserved locally

for lateral motion. Distortion due to forward motion remains complicated.

2.4 Psychophysic studies

2.4.1 Perception of slant

Domini and Caudek ([16]) carried out the experiments about perception of surface orientation under orthographic projection. The term deformation (def) is defined as

$$def = \sqrt{u_x^2 + u_y^2} \tag{2.55}$$

and the slant is shown to be related to def by

$$\sigma = \tan^{-1} \frac{def}{\beta} \tag{2.56}$$

It was found that the perceived slant magnitude is an increasing function of def, though not that of the relation expressed in Equation 2.56. The perceived slant was not significantly influenced by the simulated slant magnitudes. In another experiment, Domini and Caudek [16] found that the perceived slant increased as surface tilt varied from 0^o to 90^o . Since the axis of rotation in the experiment was vertical (frontal translation is horizontal), the tilt equals the winding angle. Therefore, we can conclude from their experiments that the perceived slant increases with the winding angle for a constant def

Cornilleau-Pérès et al. ([13]) studied the effect of projection type on the perception of slant, while avoiding the use of dot speed as a cue to slant. Results showed that the correlation between the perceived slant and the stimulus slant was significant for 3 of

the 7 subjects under perspective projection but was insignificant for all subjects under orthographic projection. Perceived slant correlated with average dot speed for both projections. However, only one configuration of surface orientation was examined, that is with a vertical rotation axis, and a normal parallel to the rotation axis (W = 90^o).

Under small field perspective projection, the optic flow can be approximated by the linear optic flow under orthographic projection. Therefore an experiment examining slant perception under small field perspective projection would produce similar results to those obtained by Domini and Caudek [16]. Using two view stimuli of planes rotating in depth, Yeow [50] and Zhong et al. [51] reported that slant information was not available with an 8^0 FOV. In this case, the reported slant was mainly a function of the average 2D speed. Thus, the reports of Domini and Caudek could be due to the average 2D dot speed. In the same studies, it is reported that, in large field perspective projection (FOV=60^o), slant perception was improved. The reported slant showed a significant positive correlation with the simulated slant. However, the slant errors were still large. Yeow [50] reported that perceived slant depended strongly on 2D dot speed but was not affected by the winding angle.

2.4.2 Perception of tilt

There have been a few psychophysics studies [16][49][51] addressing the perception of tilt from optical flow.

It is well-known that tilt is recovered more accurately than slant. Braunstein [3]reported that perceived relative depth order was consistent and accurate. Domini et al [16] and Todd et al [49]found that observers estimated tilt more accurately than slant with

multiple view stimulus under orthographic projection.

Domini et al[16] discovered that under orthographic projection with constant 3D motion, the perception of tilt was more precise if the slant magnitudes for the surfaces in a stimulus remain unchanged than the case if the slant magnitudes were different. They concluded that the perceived tilt depended on the def. A point with a greater def would be reported farther, regardless of the actual tilt. However, the average 2D image dot speed was not controlled.

This effect is stronger in small field than in large field. H. Zhong et al [51] found a strong influence of the field size and motion/orientation configuration (through the winding angle between the plane normal and the frontal translation) on tilt perception. Tilt estimation is reported to have more accuracy with large field of view. Their results support the relevance of the full flow approach in wide-field. They reported that in small field the second-order image velocity seems to be used to some extent. It is quantitatively inaccurate in that case, and the affine flow approach was given to explain the observed tilt ambiguities.

Chapter 3

Experiment 1

In this experiment, we examined the slant perception under viewpoint distortion. Our computational model showed that this distortion is equivalent to errors in the intrinsic parameters. Subjects reported the slant of a plane presented in a 2-frame image sequences in monocular vision. The orientation of the plane was indicated via the adjustment of a graphical probe, superimposed on the moving stimulus. Motion parallax was generated through a plane rotating in depth about a frontoparallel axis.

3.1 Method

3.1.1 Subjects

Three observers aged between 26 and 29 served as subjects for this experiment. Two of them are naïve subjects. The other one is the author. All of them had normal or corrected-to-normal vision.

3.1.2 Design

Different stimuli were presented in random order, defined by the following parameters

- Plane slants of $20^o, 25^o, 30^o, 35^o, 40^o$
- Plane tilts of 45^o and -45^o.
- Projection distance 0.4m (P_1) and 0.8 m (P_2).
- Winding angles: $0^o, 22.5^o, 45^o, 67.5^o, 90^o$.

Project distance refers to the distance between the screen and the projection point. There were three different viewing distances: 0.4m (V_1), 0.8m (V_2), and 1.2m (V_3) from the centre of the simulated plane to the observer. The different distances from the centre of the screen to the observer were performed alternately in random order. In total, there are 1500 trials for each subject. We examined the effects on the perception of plane slant when there were viewpoint distortion.

3.1.3 Apparatus

The stimulus patterns were generated on a PC. The virtual scene was projected onto a 22-inch monitor, placed in front of the subject. The projector resolution was 1024×768 pixels and the display refresh frequency was 85Hz. We used anti-aliasing algorithm to achieved sub-pixel accuracy, each dot covering a 4×4 area.

3.1.4 Stimulus

The image size is 0.33m in diameter. The viewing distance was 0.4m (45^o viewing angle), 0.8m (23^o viewing angle), and 1.2m (15.5^o viewing angle). The stimuli in the experiment was the perspective projections of the dotted planes. There are two types of models that have been proposed for computing 3D structure from motion: two-frame models that are restricted to the first order spatiotemporal relations between pairs of views and multiple frame model that can exploit the higher order relations of three or more views. In our experiments, two-frame models were used. The stationary subject viewed 2-view sequences of 2D images representing a rotating-in- depth plane. Each plane rotated about a frontoparallel axis. In this case the component of frontal translation T_f is orthogonal to the rotation axis.

A uniform dot density was achieved in the position of the surface corresponding to the intermediate position between the two views. This position is decided by the tilt and slant parameters as specified in the design. The $3D$ rotation angles between two views are changed according different slant to make the $2D$ dot speed stable. The duration of each view was 0.37s. The number of visible dots was 985 ± 15. Trial duration was determined by the subject and usually range around 25 s. The luminance was adjusted to 0.4 cd/m2.

A probe was presented at the centre of the screen. Subjects used the computer mouse to adjust the probe to indicate the perceived plane orientation. The probe consisted of a needle and an ellipse. The direction of the needle indicated the perceived tilt and width of the ellipse indicated the slant. A grid pattern was superimposed to the base of the probe. This square pattern enhanced the perspective through the convergence,

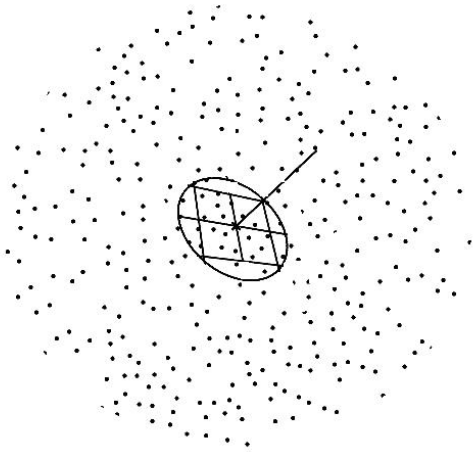

Figure 3.1: Probe

compression and skew of the squares.

3.1.5 Procedure

A chinrest with forehead support was used to fix the subject's head, and the experimental room was dark. An eye patch covered the non-dominant eye of subject to make monocular vision. The subject position was fixed with the dominant eye looking straight to the centre of the stimulus. The two views of plane were displayed repeatedly and after 3 seconds of presentation, the subject can left-click the mouse to display the probe. Subjects can display on/off the probe by left-clicking the mouse. Upon completion of the adjustment, they right-clicked the mouse, and proceeded to the next trial. The tilt and slant of the probe was recorded to a text file as the tilt and slant responses respectively.

(a) (b)

Figure 3.2: The subject in the experiment

3.1.6 2D dot speed

The 2D dot speed refers to the average 2D speed of the plane dots on the display screen. It was reported that slant is dependent on the 2D dot speed. To cancel out the effect of 2D dot speed, we choose different 3D rotation angles for different slant so that all stimulus have equal 2D dot speed. The corresponding rotation angles were given in Table 3.1.

Slant (degree)	Rotation Angle in P_1 (degree)	Rotation Angle in P_2 (degree)
20	2.92	3.32
25	2.39	2.63
30	2	2.16
35	1.71	1.81
40	1.46	1.53

Table 3.1: Rotation angles for different slants and projection distances

3.2 Result

The data (the reported slant and tilt) was analyzed using non-parametric tests, in particular, the Spearman's ranked correlation. Non-parametric testing was used because our data were not necessarily Gaussian, in particular the slant variable, which was bounded between 0^o and 90^o.

3.2.1 Verbal report

All subjects reported that the stimulus is not a flat plane but a curved surface. This verbal report was also found out in Zhong et al[51]. They did not explain why this distortion happened but they mentioned about their research in curved surface which shown an offset of the reported curvature towards convexity when viewing motion parallax. In this experiment, when examining slant perception, subjects reported that it was very difficult to choose the right orientation of the plane. They also claimed that they did not have very high confidence in their choices

3.2.2 Analysis of slant responses

Slant responses were analyzed by computing the Spearman's ranked correlation between the simulated slant and the reported slant. When the projection distance was 0.8m, all the correlations were negative. Furthermore, subject LS reported a very poor perceived slant. All correlations between the reported and stimulus slant of LS in different viewpoint and projection distance are negative whereas negative correlations also appeared in the other two subjects. Responses from two other subjects showed

that the correlation was positive and significant when projection distance is 0.4 m. In this case, the correlation was still significant when there were viewpoint distortion. Table 3.3 shows the results of absolute slant error (the difference between simulated slant and reported slant) from the two subjects. The results were similar in all the three viewing distances.

Subject	P_1			P_2		
	V_1	V_2	V_3	V_1	V_2	V_3
LS	-0.05	-0.04	-0.16	-0.055	-0.068	-0.124
NL	0.157**	0.198**	0.164**	-0.191**	0.058	0.052
TD	0.103**	0.364**	0.313**	-0.125**	-0.047	-0.024

Table 3.2: Spearman's ranked correlation between the simulated slant and the reported slant. Those correlations with asterisks ** are significant at $p < 0.01$ (N=250).

Viewing distance(m)	Mean of absolute slant error(deg)
0.4	8.16
0.8	6.58
1.2	7.52

Table 3.3: Absolute slant error when projection distance = 0.4m

3.2.3 Analysis of tilt responses

Tilt response were analyzed, and a depth reversal was recorded each time the absolute error in tilt exceeded 90^o. Table 3.4 showed that in P_1, there were almost no depth reversal due to the large FOV. The viewpoint distortion did not lead to a depth reversal. However, in P_2, even when the distant viewpoint was 0.4m, under which the apparent

FOV is large, depth reversal still occurred in this case.

P_1			P_2		
V_1	V_2	V_3	V_1	V_2	V_3
1	1	2	9	20	29

Table 3.4: Number of tilt reversal in a total of 500 trials under each condition

3.2.4 Discussion

Our results showed that human subjects could not recover the slant of a randomly dotted plane when FOV is small at 23^o (projection distance = 0.8m in our experiment). The response from one of the three subjects showed weak negative correlation between the reported slant and the simulated slant, the Spearman's correlation ranging between -0.124 (p=0.051) and -0.055 (p=0.337). The other two subjects even reported a significant negative correlation between the perceived slant and the stimulus slant when there was viewpoint distortion (viewpoint distance = 0.4m). These corresponding Spearman's correlations were -0.191 and -0.125 with $p < 0.01$.

In contrast, human subjects could partly recover the slant of a randomly dotted plane when FOV is large at 45^o (in our experiment, this corresponds to a projection distance = 0.4m). The results from two of the three subjects showed a significant correlation between the reported slant and the simulated slant. When there was no viewpoint distortion (viewpoint distance = 0.4m), these correlations were 0.157 and 0.103 ($p < 0.01$).

Besides, the viewpoint distortion has no significant effect when the human subjects

could recover the slant. The slant responses from the two subjects above were still significantly correlated to stimulus slant when there was viewpoint distortion. The corresponding Spearman correlations were between 0.164 and 0.364 ($p < 0.01$). Using ANOVA to analyze absolute slant error result from these two subjects, there was no significant difference under viewpoint distortion (Sig=0.494). The mean of absolute slant errors(the difference between simulated slant and reported slant)were 8.16^o when there was no viewpoint distortion and were 6.58^o and 7.52^o when there was viewpoint distortion.

In examining the perception of the slant of a moving plane, our results also agree with those reported by Domini and Caudek[16]. In their experiments, they used orthographic projection with a FOV = 9.6^o. This configuration eliminated all second order optic flow information. They reported that the perceived slant was not correlated to the simulated plane. In our experiments, even when we used the perspective projection with a FOV=23^o, we cannot find a significant correlation between the reported slant and the simulated slant. Only when increasing the FOV to 45^o, there are significant correlation between the reported slant and the actual slant of the moving plane.

In conclusion, in this experiment, when the viewpoint distance = 0.8m, all the reported slant was not correlated with the simulated slant. We could only use the slant response when the viewpoint distance = 0.4m. Even then, we cannot find out any significant effect of viewpoint distortion on the perception of slant. Thus, Experiment 1 might not be conclusive as to whether viewpoint distortion affects slant perception or not. The only large FOV condition that we could analyze was not under viewpoint distortion (viewing distance=0.4m, projection distance=0.4m). The lack of sufficient FOV (whether real or apparent) could affect the recovery of slant. Therefore, experiment 2

was designed to examine the effect of viewpoint distortion on slant perception in large FOV when the viewpoint distance was fixed at 0.4m and the projection distance was changed between 0.3 & 0.4m.

Chapter 4

Experiment 2

In Experiment 1, we examined if viewpoint distortion affects the ability of human subjects to perceive the slant of a dotted plane. The result showed that viewpoint distortion did not prevent the slant recovery in large FOV under viewpoint distortion. However, in many other cases, the FOV of human subjects was relatively small (15.5^o or 23^o), under which the results were not conclusive. Thus, in Eperiment 2, we carried out another set of experiment with a larger FOV to examined in more details how the viewpoint distortion might affect slant perception.

4.1 Method

4.1.1 Subjects

Three observers aged between 25 and 30 served as subjects for this experiment. Two of them are naïve subjects. The other one is the author. All of them had normal or

corrected-to-normal vision.

4.1.2 Design

Different stimuli were presented in random order, defined by the following parameters

- Plane slants of $20^o, 25^o, 30^o, 35^o, 40^o$
- Plane tilts of 45^o and -45^o.
- Projection distance 0.3m (P_1) and 0.4 m (P_2).
- Winding angles: $0^o, 22.5^o, 45^o, 67.5^o, 90^o$.

The distance from the centre of the screen to the observer were 0.4m. In total, there were 750 trials for each subject. We examined the effects on the perception of the slant of a plane when there was viewpoint distortion, including how winding angle affected the absolute slant error when there was viewpoint distortion.

Table 4.1 showed angle of the rotating-in-depth of the dotted plane in our experiments. With these values, the 2D dot speed was kept at a constant.

4.1.3 Stimulus and Procedure

The stimuli and procedure were similar to that of experiment 1.

Slant (degree)	Rotation Angle in P_1 (degree)	Rotation Angle in P_2 (degree)
20	2.4	2.92
25	2.1	2.39
30	1.87	2.0
35	1.62	1.71
40	1.4	1.46

Table 4.1: Rotation angle for different slant and projection distance

4.2 Result

4.2.1 Analysis of slant responses

Slant responses were analyzed by computing Spearman's ranked correlation between the simulated slant and the reported slant. Subject CH reported a poor perception of slant. In both projection distances, correlations between the reported and the stimulus slant of CH are positive but not significant. Responses from two other subjects showed that the correlation was positive and significant in both projection distance. The correlation was still significant when there were viewpoint distortion.

Figure 4.1 showed a positive relation between the reported slant and the simulated slant, with large over-estimatation of slant. There was no significant difference in the reported slant distribution when there was viewpoint distortion. Only when slant was large, (in our experiment, it was 40^o) there was a small difference. As shown in Figure 4.1, in viewpoint distortion case, when the simulated slant increased from 35^o to 40^o, reported slant decreased.

Subject	P1	P2
NL	0.417**	0.324**
LY	0.228**	0.229**
CH	0.082	0.0806
All subjects	0.105**	0.163**

Table 4.2: Spearman's ranked correlation between the simulated slant and the reported slant. Those correlations with asterisks ** are significant at $p < 0.01$ (N=360).

Tilt(deg)	P1	P2
45	0.201*	0.0.254**
-45	0.179*	0.224**

Table 4.3: Spearman's ranked correlation between the simulated slant and the reported slant of subject CH. Those correlations with asterisks ** are significant at $p < 0.01$. Those correlations with asterisks * are significant at $p < 0.05$ (N=180).

4.2.2 Effect of winding angle on reported slant

The first and second order optic flow coefficients vary with the winding angle. It has been shown that winding angle affected both reported slant and tilt percept. Therefore we tested how winding angle affected absolute slant error when there was viewpoint distortion. Using the data of subjects NL an KY, Figure 4.2 showed that absolute slant error decreased when winding angle increased or decreased toward 45^o whether under or not under viewpoint distortion.

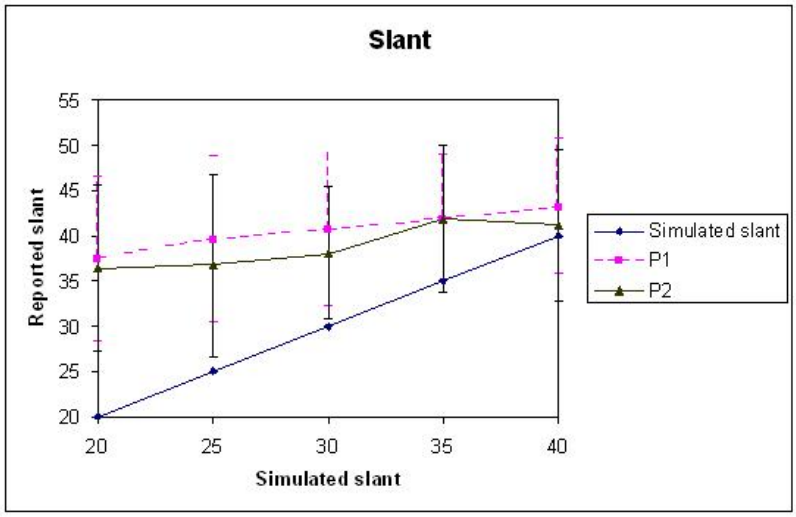

Figure 4.1: Reported slant

4.2.3 Discussion

The verbal response of this experiment was similar with the one of Experiment 1. Subjects reported that the simulated plane was curved. They were not confident in their choices. However, in this experiment, when subject were at a viewpoint distance of 0.4 m with FOV = 45^o, the reported slant was highly correlated with the simulated slant. The absolute slant error was still very large, the mean of absolute slant error being 11.6^o. Two of the subjects reported a significant correlation, with correlation coefficients from 0.228 to 0.324 ($p < 0.01$). Subject CH reported a positive but not significant correlation. However when examining CH's reported slant under a particular setting of tilt (Table 4.3), the reported slant was significantly correlated with the simulated slant. When tilt = -45^o, correlation coefficients were 0.179(p=0.02) and

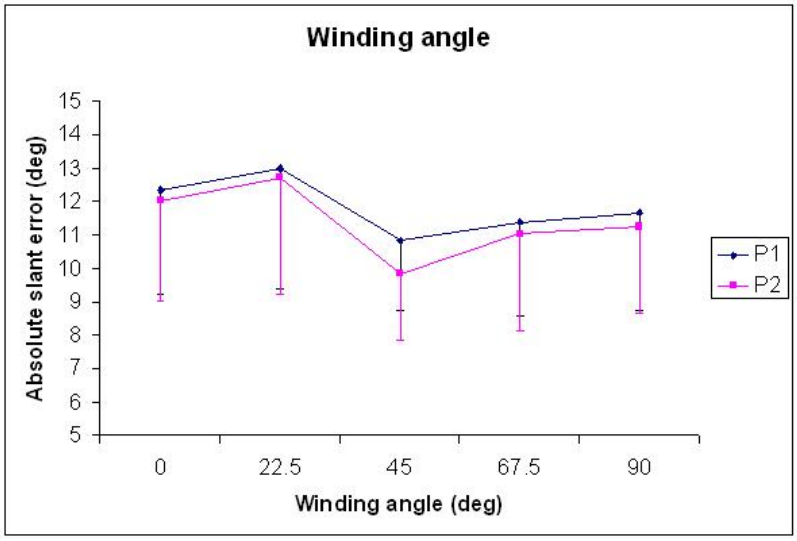

Figure 4.2: The absolute slant error against the winding angle

0.254 (p=0.002); when tilt = 45^o, correlation coefficients were 0.201(p=0.015) and 0.224 (p=0.007)

Keeping the viewpoint distance and reducing the projection distance (ie a larger simulated FOV but with viewpoint distortion) did not help significantly in increasing the perception of slant. In fact, it introduced a weak distortion when the slant was large. When the simulated slant increased from 35^o to 40^o, the mean of the reported slant slightly decreased from 41.82^o to 41.18^o.

The effect of winding angle on absolute slant error did not change under viewpoint distortion. When there was no viewpoint distortion, absolute slant error decreased from 12.33^o to 10.82^o when winding angle increased from 0^o to 45^o, and increased to 11.64^o when winding angle increased to 90^o. When there was viewpoint distortion, similarly, absolute slant error also decreased from 12.03^o to 9.84^o when winding angle = 45^o, and increased to 11.24^o when winding angle =90^o. It is obvious that, under viewpoint distortion, absolute slant error distribution against winding angle still keeps the same shape as that under no viewpoint distortion.

In conclusion, in the case of large FOV and there was viewpoint distortion , the effect of viewpoint distortion to slant perception is not significant.

Chapter 5

Experiment 3

In Experiment 1, we examined if viewpoint distortion effects the ability of perceive the slant of a dotted plane. The result showed that viewpoint distortion did not prevent the slant recovery in large FOV under viewpoint distortion. However, in these cases, the FOV of human subjects was relatively small (15.5^o or 23^o), except for the case when the viewing coincides with the projection point, under which the FOV is moderately large (45^o). Thus in Eperiment 2, we carried out another set of experiment with a larger FOV to examined in more detail hows the viewpoint distortion affected slant perception.

5.1 Method

5.1.1 Subjects

Three observers aged between 26 and 28 served as subjects for this experiment. Two of them are naïve subjects. The other one is the author. All of them had normal or corrected-to-normal vision.

5.1.2 Design

Different stimuli were presented in random order, defined by the following parameters

- Plane slants of 30^o
- Plane tilts of $-170^o, 160^o ... -10^o, 0^o, 10^o, ...170^o, 180^o$
- Projection distance of 0.4m (P_1) and 0.8 m (P_2).
- Winding angles: $15^o, 30^o, 45^o, 60^o, 75^o$.

There were three different viewing distances: 0.4m (V_1), 0.8m (V_2), and 1.2m (V_3) from the centre of the simulated plane to the observer. The different distances from the centre of the screen to the observer were performed alternately in random order. In total, there are 1080 trials for each subject. We examined the effects on the perception of plane tilt when there were viewpoint distortion.

5.1.3 2D dot speed

As reported by Zhong et al [51] , 2D dot speed helps decrease the absolute tilt error. Again, to cancel out the effect of 2D dot speed, we chose different 3D rotation angle for different projection distance. When the projection distance was 0.4m, the 3D rotation angle was 2.0^o. When the projection distance was 0.8m, the rotation angle was 2.16^o.

5.1.4 Stimulus and Procedure

The stimulus and procedure was similar to that in experiment 1.

5.1.5 Data analysis

We removed the ambiguity on the tilt sign (tilt reversal) by calculating the percentage of trials where the unsigned tilt error ranged between 90^o and 180^o. Having corrected the responses for this ambiguity, we then used the corrected absolute tilt error as a measure of the performance, ranging between 0^o and 90^o. Since most distributions were not strictly normal (for instance the absolute tilt error is bounded by the value 0), we used non-parametric tests, we compared independent samples with the Mann−Whitney U test (MWU).

5.2 Result

5.2.1 Verbal report

In experiment 3, about tilt perception with a fixed slant, subjects seemed to be able to choose more easily the orientation of the plane, even under viewpoint distortion. They reported that these were quite simple tasks.

5.2.2 Effect of viewpoint distortion on the reported tilt sign

Table 5.1 showed that FOV affected strongly the reported tilt sign. In large FOV (45^o in our case), tilt reversals were only less than 0.02%. When FOV=23^o, titl reversals were about 5%. In both projection distances, viewpoint distortion did not affected significantly the amount of depth reversal. For example, at FOV=23^o, the number of tilt reversal was 35 when there was no viewpoint distortion (viewing distance=projection distance=0.8m). When there was viewpoint distortion (viewing distance = 0.4m), the number of tilt reversal was 33.

P_1			P_2		
V_1	V_2	V_3	V_1	V_2	V_3
4	8	1	33	35	25

Table 5.1: Number of tilt reversal trials in a total of 540 trials for each condition

5.2.3 Effect of viewpoint distortion on absolute tilt error

The average absolute tilt error, as presented in Figure 5.1, is almost unchanged under viewpoint distortion in both projection distances. There are significant differences in the absolute tilt error among subjects. Subject DC reported average absolute tilt error from 22.3^o to 26^o when subject NL reported average absolute tilt error from 9.9^o to 13.2^o. But for each subject, the differences when there was distortion viewpoint were not significant. We had no evidence showed that there was significant difference in absolute tilt error when there was viewpoint distortion. (MWU test Z ranges from -1.71 to -0.33 with $p > 0.05$).

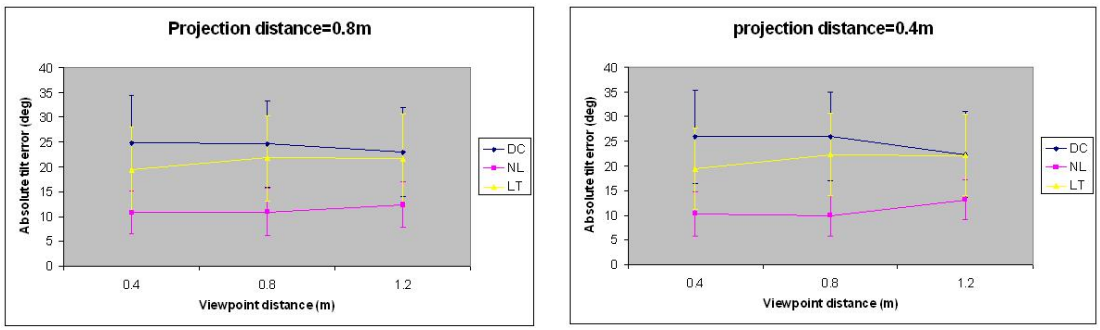

(a) (b)

Figure 5.1: Absolute tilt error under viewpoint distortion

5.2.4 Effect of winding angle and viewpoint distortion on the absolute tilt error

Figure 5.2 showed that the average absolute tilt error increased dramatically as winding angle increased under all projection distances and viewpoint distances. It means that the viewpoint distortion did not change the influence of winding angle on the absolute tilt error. Two of the three subject reported significant correlation between absolute tilt error and winding angle under all projection distances and viewpoint distances: the Spearman's ranked correlation coefficient ranging from 0.17 to 0.40 ($p < 0.01$).

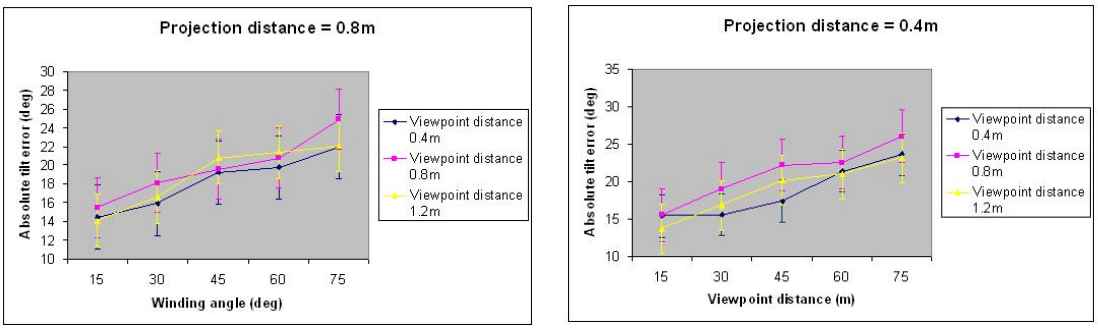

(a) (b)

Figure 5.2: The absolute tilt error against the winding angle

5.2.5 Discussion

In terms of tilt perception, our results agree with those obtained by Domini and Caudek[16]. The perceived tilt reported by these authors showed a mean error that can be estimated at around $10^o - 15^o$. It is smaller than the mean error that we find in

Experiment 3. This could be due to the choice of the direction of the rotation, which is changed in our experiments, and fixed in theirs. In their case, the reported tilt might be perceived better by an a priori knowledge (built up during experimental sessions) of the motion direction. When there was viewpoint distortion, the absolute tilt error was not affected significantly. The average absolute tilt error only changed $1-2^o$ when there was viewpoint distortion

We also confirmed the result obtained by Zhong et al[51]. They reported that the absolute tilt error increased when winding angle increased. Our results display strong influence of winding angle on the perception of the tilt of a moving plane. However, they found a very different effect of winding angle on tilt error in large FOV and small FOV with the later showing a stronger sensitive to the influence of winding angle. In our case, when changing the projection point, such that the FOV is changed, the results are not significantly changed. In their experiment, the difference in FOV settings was very large: 60^o versus 8^o. In our cases,the difference is 45^o versus 23^o. These FOVs in our experiments might still give enough information for the processing of second-order optic flow, therefore resulting in a lesser sensitivity with the winding angle. In our experiment, the winding angle effect to absolute tilt error was kept when there was viewpoint distortion. The correlation between winding angle and absolute tilt error was significant positive.

In conclusion, our results showed that the viewpoint distortion might not significantly affect the reported tilt. Under different viewing distances and project distances, the tilt perception seemed not change. It means that viewpoint distortion in our experiment did not change the depth order. Furthermore, the results from Experiment 1 and Experiment 2 suggested that viewpoint distortion in these two experiments might not

significantly affect slant perception. It is such an interesting question why viewpoint distortion did not affect to tilt and slant perception in our experiments. In the next chapter, we would provide the computational modeling of viewpoint distortion in our experiment and explanation for our experimental results.

Chapter 6

Computational Interpretation

Here, we examine the optic flow equations for a plane moving in the 3D space, under viewpoint distortion. In particular, we examine the impact on the solutions for the tilt and slant of the plane. We then explain how human subjects might adapt well to viewpoint distortion.

6.1 Viewpoint distortion is equivalent to errors in intrinsic parameters

In this section, we provide the computational model for viewpoint distortion. This distortion is shown to be equivalent to errors in the intrinsic parameters . We use subscripts p, v to represent quantities associated with the projection point and the viewpoint. The distances (along the Z axis) from the screen to the projection point and to the viewpoint are D_p and D_v, respectively. Assume that the projection point and the actual viewpoint all lie on the Z axis. A world point (X, Y) on the screen

would project to the image point (x_p, y_p) for a subject at the projection point and the image point (x_v, y_v) for a subject at the actual viewpoint:

$$x_p = \frac{fX}{D_p} \tag{6.1}$$

$$y_p = \frac{fY}{D_p} \tag{6.2}$$

$$x_v = \frac{fX}{D_v} = \frac{x_p}{k} \tag{6.3}$$

$$y_v = \frac{fY}{D_v} = \frac{y_p}{k} \tag{6.4}$$

where

$$k = \frac{D_v}{Dp} \tag{6.5}$$

The motion flow in the subject's visual system at the actual viewpoint is related to the "true" motion flow at the projection point by:

$$u_v = \dot{x_v} = \frac{\dot{x_p}}{k} \tag{6.6}$$

$$v_v = \dot{y_v} = \frac{\dot{y_p}}{k} \tag{6.7}$$

Equations (6.6), (6.7) suggest that the flow perceived at the viewpoint is scaled by a factor k compared with the corresponding flow at the projection point. The flow at projection point is given by the well-known equation:

$$\begin{aligned} u_p &= \tfrac{W}{Z}\left(x_p - f\tfrac{U}{W}\right) + \alpha\tfrac{x_p y_p}{f} - \beta\left(\tfrac{x_p^2}{f} + f\right) + \gamma y \\ v_p &= \tfrac{W}{Z}\left(y_p - f\tfrac{V}{W}\right) - \beta\tfrac{x_p y_p}{f} + \alpha\left(\tfrac{y_p^2}{f} + f\right) - \gamma y \end{aligned} \tag{6.8}$$

Expanding the horizontal component of the flow u_v at the viewpoint in equation (6.6) and bringing in equation (6.8), we obtain:

$$\begin{aligned} u_v = {} & \frac{W}{Z}\left(x_v - \frac{fU}{kW}\right) + \alpha\frac{x_v y_v}{\frac{f}{k}} \\ & -\beta\left(\frac{x_v^2}{\frac{f}{k}} + \frac{f}{k}\right) + \gamma y_v \end{aligned} \tag{6.9}$$

Similar expression can be written for the vertical flow v_v. From equation (6.9), we see that the optical flow obtained by a subject at the actual viewpoint is one that stems from the same $3-D$ motion at the projection point with a modified focal length:

$$f_v = \frac{f}{k} \tag{6.10}$$

It means that the viewpoint distortion in our experiments is equivalent to a distortion in the focal length.

6.2 Optical flow equations for local surface patch

When using optical flow to reconstruct depth from motion, if the focal length is known and fixed, focal length can be set as $f = 1$ without loss of generality. However, when the focal length is changed,without corresponding update in the estimate for f, such error will affect the depth reconstruction process. In the following, optical flow in a local surface patch will be re-derived with explicit representation of the focal length.

We introduce a method to map a point on the image plane (x, y) to the point on the surface in the scene. Actually, Z^{-1} will be expressed in term of (x, y), the focal length f and the surface structure. This method was used by M.Subbarao []. However in his work, the focal length f was assumed to be equal to 1 and therefore did not appear in his equations.

Assuming that the surface is smooth and is given by $Z = f(X, Y)$, we can expand the surface equation in a Taylor series:

$$Z = Z_0 + Z_X X + Z_Y Y + Z_{XX} X^2 + Z_{XY} XY + Z_{YY} Y^2 + O_3(X, Y) \tag{6.11}$$

Replacing X,Y by:

$$\begin{aligned} X &= \frac{Zx}{f} \\ Y &= \frac{Zy}{f} \end{aligned}$$

Z can be expressed in terms of the image coordinate x, y and the focal length f:

$$Z = Z_0 + \frac{Z}{f}(Z_X x + Z_Y y + \frac{Z}{f}(Z_{XX}x^2 + Z_{XY}xy + Z_{YY}y^2 + \frac{Z}{f}O_3(x,y))) \qquad (6.12)$$

To eliminate the second and higher order terms of Z, we recursively replace the appropriate Z in the right hand side of the above equation by the entire right hand side of equation:

$$\begin{aligned} Z &= Z_0 + \frac{Z}{f}(Z_X x + Z_Y y + \frac{1}{f}(Z_0 + \frac{Z}{f}(Z_X x + Z_Y y + \\ &\quad \frac{Z}{f}(Z_{XX}x^2 + Z_{XY}xy + Z_{YY}y^2 + \frac{Z}{f}O_3(x,y)))) \times \\ &\quad \times(Z_{XX}x^2 + Z_{XY}xy + Z_{YY}y^2 + \frac{Z}{f}O_3(x,y))) \end{aligned}$$

Rearranging the term of Z, using $O_3(x, y)$ to denote all third and higher order terms:

$$\begin{aligned} Z &= Z_0 + \frac{Z}{f}(Z_X x + Z_Y y + \frac{1}{f}(Z_0 Z_{XX}x^2 + Z_0 Z_{XY}xy + Z_0 Z_{YY}y^2 + Z_0\frac{Z}{f}O_3(x,y)) + \\ &\quad + \frac{Z}{f}(Z_X x + Z_Y y + \frac{Z}{f}(Z_{XX}x^2 + Z_{XY}xy + Z_{YY}y^2 + \frac{Z}{f}O_3(x,y))) \times \\ &\quad \times(Z_{XX}x^2 + Z_{XY}xy + Z_{YY}y^2 + \frac{Z}{f}O_3(x,y))) \\ &= Z_0 + \frac{Z}{f}(Z_X x + Z_Y y + \frac{1}{f}(Z_0 Z_{XX}x^2 + Z_0 Z_{XY}xy + Z_0 Z_{YY}y^2 + O_3(x,y)) \\ &= Z_0 + Z(\frac{Z_X}{f}x + \frac{Z_Y}{f}y + \frac{Z_0}{f}\frac{Z_{XX}}{f}x^2 + \frac{Z_0}{f}\frac{Z_{XY}}{f}xy + \frac{Z_0}{f}\frac{Z_{YY}}{f}y^2 + O_3(x,y)) \end{aligned}$$

Bringing Z from the right hand side to the left hand side, we have:

$$Z = Z_0(1 - \frac{Z_X}{f}x - \frac{Z_Y}{f}y - \frac{Z_0}{f}\frac{Z_{XX}}{f}x^2 - \frac{Z_0}{f}\frac{Z_{XY}}{f}xy - \frac{Z_0}{f}\frac{Z_{YY}}{f}y^2 - O_3(x,y))^{-1} \qquad (6.13)$$

The optical flow (u, v) for a general scene structure is given by:

$$\begin{aligned} u &= \frac{f}{Z}(-U - \beta Z + \gamma Y) - f\frac{X}{Z}(\frac{-W - \alpha Y + \beta X}{Z}) \\ &= \frac{-fU}{Z} - f\beta + y\gamma + x\frac{W}{Z} + xy\frac{\alpha}{f} - x^2\frac{\beta}{f} \\ &= \frac{1}{Z}(xW - fU) + (-x^2\frac{\beta}{f} + xy\frac{\alpha}{f} + y\gamma - f\beta) \end{aligned}$$

Replacing Z^{-1} for the case of a second order surface using equation (6.13):

$$\begin{aligned} u &= (\frac{xW}{Z_0} - \frac{fU}{Z_0})(1 - \frac{Z_X x}{f} - \frac{Z_Y y}{f} - \frac{1}{2}\frac{Z_0 Z_{XX} x^2}{f^2} - \frac{1}{2}\frac{Z_0 Z_{YY} y^2}{f^2} \\ &\quad -\frac{Z_0 Z_{XY} xy}{f^2}) + (-x^2\frac{\beta}{f} + xy\frac{\alpha}{f} + y\gamma - f\beta) \\ u &= (-f\frac{U}{Z_0} - f\beta) + (\frac{W}{Z_0} + \frac{U}{Z_0}Z_X)x + (\gamma + \frac{U}{Z_0}Z_Y)y + \\ &\quad +\frac{1}{2}\frac{1}{f}(-2\frac{W}{Z_0}Z_X - 2\beta + \frac{U}{Z_0}Z_{XX})x^2 + \frac{1}{2}\frac{1}{f}\frac{U}{Z_0}Z_{YY}y^2 + \\ &\quad +\frac{1}{f}(-\frac{W}{Z_0}Z_Y + \frac{U}{Z_0}Z_{XY} + \alpha)xy \end{aligned}$$

The first and second order derivatives of the optical flow can be extracted as follow:

$$u_0 = -f(\frac{U}{Z_0} + \beta) \tag{6.14}$$

$$u_x = \frac{W}{Z_0} + \frac{U}{Z_0}Z_X \tag{6.15}$$

$$u_y = \gamma + \frac{U}{Z_0}Z_Y \tag{6.16}$$

$$u_{xx} = \frac{1}{f}(-2\frac{W}{Z_0}Z_X - 2\beta + UZ_{XX}) \tag{6.17}$$

$$u_{xy} = \frac{1}{f}(-\frac{W}{Z_0}Z_Y + UZ_{XY} + \alpha) \tag{6.18}$$

$$u_{yy} = \frac{1}{f}(UZ_{YY}) \tag{6.19}$$

From the above equations, changing f will lead to a change in $u_0, u_{xx}, u_{xy}, u_{xx}$ but no change in u_x, u_y. With similar method, we have the same conclusion with v:

$$v_0 = -f(\frac{V}{Z_0} + \alpha) \tag{6.20}$$

$$v_y = \frac{W}{Z_0} + \frac{W}{Z_0} Z_Y \tag{6.21}$$

$$v_x = -\gamma + \frac{W}{Z_0} Z_X \tag{6.22}$$

$$v_{yy} = \frac{1}{f}(-2\frac{W}{Z_0} Z_Y + 2\alpha + Y Z_{YY}) \tag{6.23}$$

$$v_{xy} = \frac{1}{f}(-\frac{W}{Z_0} Z_X + V Z_{XY} - \beta) \tag{6.24}$$

$$v_{xx} = \frac{1}{f}(U Z_{XX}) \tag{6.25}$$

6.3 Tilt and slant

In our experiments, lateral motion is studied because it produces good results in terms of depth from motion parallax. It comprises a rotation $\mathbf{R} = (0, \beta, 0)$ and a translation $\mathbf{t} = (U, 0, W)$, where $U >> W$.

With this special motion, the optical flow derivatives are simplified:

$$u_0 = 0$$

$$v_0 = 0$$

$$v_x = 0$$

With these optic flow derivatives, the tilt and slant can be readily derived:

$$\tau = \tan^{-1} \frac{u_y}{u_x - v_y} \tag{6.26}$$

$$\sigma = \tan^{-1} \sqrt{\frac{f^2 u_{xy}^2 (u_y^2 + (u_x - u_y)^2)}{u_y^2 v_y^2}} \tag{6.27}$$

As a result of equation (6.26), the tilt can be recovered from first order optical flow only. Note that the focal length is not necessary in recovering tilt. Under viewpoint distortion stimulated in our experiments, only the focal length is changed. This distortion therefore should not affect significantly the tilt estimation. In contrast, to obtain

the slant, second order components and focal length information are necessary. It is the reason why observers estimate the tilt more accurately than the slant in reported experiments; in our case, with the change in focal length, the performance of slant estimation might be further worsened.

6.4 Iso-distortion framework

The iso-distortion framework was first introduced by Cheong et al. [6]. The iso-distortion framework seeks to understand the distortion due to some errors in the estimated camera parameters. In this framework, the estimated depth $\hat{Z}$ is described to be related to the actual depth Z as $\hat{Z} = DZ$ with D being the distortion factor (the bracket term in equation (2.53) in chapter 2).

In our experiments, slant estimation is significantly affected by both the motion estimates and the focal length estimate. We now apply the iso-distortion framework to examine the tilt and the slant recovery from motion under viewpoint distortion. In our experiments, the focal length is fixed but unknown and the motion is a lateral motion. In this case, the distortion factor D is given by Cheong and Xiang [9]:

$$D = \frac{\hat{f}_v \hat{U}}{f_v U + \left(\beta f_v - \hat{\beta}\hat{f}_v\right) Z} = \frac{\hat{f}_v \hat{U}}{U\frac{f_p}{k} + \left(\beta \frac{f_p}{k} - \hat{\beta}\hat{f}_v\right) Z} \tag{6.28}$$

6.5 Depth distortion arising from errors in estimation of 3-D motion and intrinsic parameters

6.5.1 Explanation using optical flow equations

6.5.1.1 Tilt estimation

Our psychphysics result confirm the well-known better estimation of the tilt than the slant of a moving plane. They also agree with those obtained by H.Zhong et al (2006) in terms of the influence of winding angle W on the ability to report the tilt. With regards to the concern of this work, namely, under viewpoint distortion, it is found that the estimation of the tilt is still reliable in accordance with the predictions made in section 5.3. When the viewpoint is different from the projection point, the mean error of the reported tilt is approximately the same as the mean error of reported tilt of the subject seated at the projection point. Since the viewpoint distortion in our experiment is equivalent to a change in the focal length, the results support the conjecture that subjects do not need focal length information to recover the tilt of a plane. (Equation(6.26)).

Since viewpoint distortion does not affect tilt estimation, it means that when we design an HMD devices for applications where users only need ordinal depth (i.e. tilt) to carry out the tasks, it is acceptable to ignore the viewpoint distortion. The same conclusion applies for viewers in cinema: their perceived ordinal depth does not depend on the distance from their seats to the screen, and this might allow them an adequate appreciation of the layout of the scene portrayed in the cinematic pictures.

6.5.1.2 Slant estimation

In contrast to tilt estimation, equation (6.27) shows that slant recovery is a much more difficult task. It requires the focal length information and the second order derivatives of optical flow. In our experimental results, the effect of the change in focal length is not significant. Our result show that in large field of view, under viewpoint distortion, there is almost no difference in the performance on slant perception. There is only a small difference when the actual plane slant is big (slant=40).

Equation (6.27) does not seem to help us to explain clearly our experiment results. It predicts the viewpoint distortion will add more errors to the perceived slant. In the next section, we will use the iso-distortion framework to examine how the viewpoint distortion might effect the slant recovery.

6.5.2 Explanation using iso-distortion framework

6.5.2.1 Tilt estimation

The distortion factor expressed in equation (6.28) has the form $\frac{1}{a+bZ}$, where $a = \frac{f_v U}{\hat{f}_v \hat{U}}$ and $b = \frac{\beta f_v - \hat{\beta}\hat{f}_v}{\hat{f}_v \hat{U}}$ are constants for all the scene points. Such distortion has the property that it preserves the depth order of any two recovered depths $\hat{Z}_1$ and $\hat{Z}_2$ under certain minimal conditions that are likely to hold (see Cheong and Xiang [9] for details). For instance, if $Z_1 > Z_2$, it can be readily shown that, given either of the following conditions, depending on the sign of a:

- $(a + bZ_1)(a + bZ_2) > 0$ if $a > 0$, or

- $(a + bZ_1)(a + bZ_2) < 0$ if $a < 0$

the transformation $\hat{Z} = DZ$ preserves the depth order of the two points, that is, $\hat{Z}_1 > \hat{Z}_2$. Since $a = \frac{f'_v U}{\hat{f}'_v \hat{U}}$, the condition $a > 0$ means that $f_v U$ and $\hat{f}_v \hat{U}$ have the same sign. This condition can easily be met by human visual system; thus we can just focus on the first condition. The requirement $(a + bZ_1)(a + bZ_2) > 0$ simply means that the two estimated depths should have the same sign since $\hat{Z}_1 = \frac{Z_1}{a+bZ_1}$, $Z_2 = \frac{Z_2}{a+bZ_2}$. This condition can be easily assured: just check the sign of $\hat{Z}_1$ and $\hat{Z}_2$. If they are of the same sign, the depth order of $\hat{Z}_1$ and $\hat{Z}_2$ is correct; otherwise, just reverse the depth order. It means that the tilt or the ordinal depth is perceived well under viewpoint distortion.

6.5.2.2 Slant estimation

Equation (6.28) indicates that under viewpoint distortion, the distortion factor changes according to the following factors:

- $\hat{f}_v$ is the focal length estimated by human.
- f_v is the actual focal length that is changing under viewpoint distortion.
- $\hat{U}, \hat{\beta}$ are the translation and rotation estimated by the human visual systems.
- U, β are the actual translation and rotation respectively.

Under viewpoint distortion, f_v is changed. Meanwhile, D is also strongly influenced by human visual systems's estimates of the motion and the focal length. All these estimates can combine to generate a rather similar distortion contour distribution

compared to that under no viewpoint distortion. Figure (6.1) showed a case where $\hat{f}_v = 2, \hat{U} = 12, U = 10, \beta = -0.002, \hat{\beta} = 0.0008$. It can be observed that when f_v changed from 1.0 to 1.4, equivalent to a 40% change in viewpoint distance, the distortion contour distributions were not significantly different. Our experimental results seemed to correspond to this case where there was almost no difference in the distortion contour distribution.

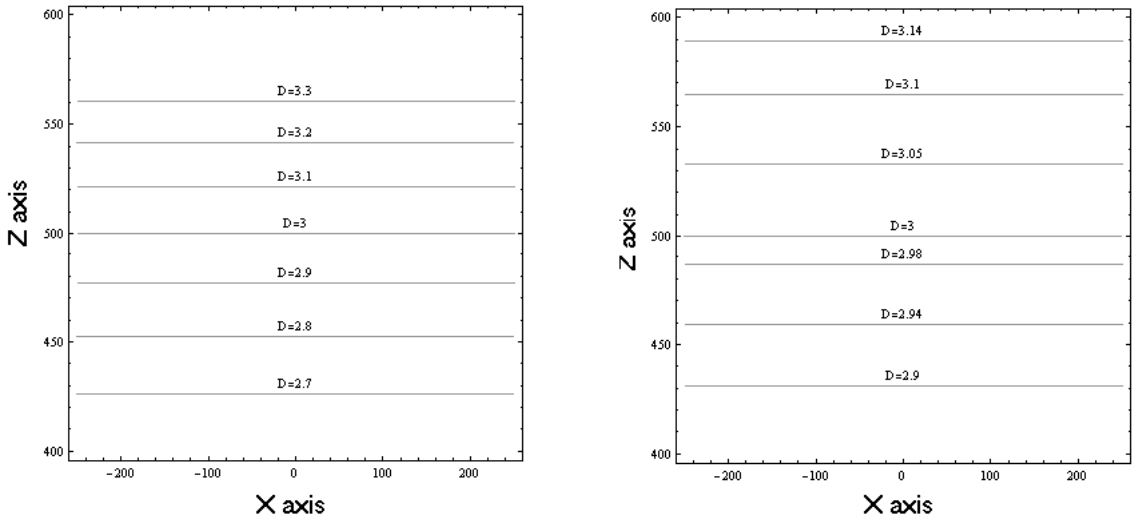

(a) (b)

Figure 6.1: Families of iso-distortion contours for lateral motion obtained by intersecting the iso-distortion surfaces with the xZ-plane. $\hat{f}_v = 2, \hat{U} = 12, U = 10, \beta = -0.002, \hat{\beta} = 0.0008$,. (a) Actual $f_v = 1.0$ (b) Actual $f_v = 1.4$

Chapter 7

Conclusion and Future work

7.1 Conclusion

In this thesis, we presented the computational theories and psychophysical results on the recovery of tilt and slant from monocular lateral motion under viewpoint distortion. The computational modeling shows that the viewpoint distortion could be regarded as an equivalent distortion in the intrinsic camera parameters. In our experimental design, we focus on the case where the viewpoint distortion is equivalent to a distortion in the focal length. The optical flow obtained by a subject at the actual viewpoint is one that stems from the same $3-D$ motion at the projection point but with a modified focal length $f_v = \frac{f}{k}$ (Equation 6.10)

Conventionally, the focal length is often set as f=1 if it is known and fixed. With viewpoint distortion, the computational modeling showed that the focal length is changed. Thus we re-derived, with explicit representation of the focal length, the optical flow of a local surface patch. The relationship between the optic flow derivatives, and the

tilt and slant are obtained. Based on these equations, we predict that the focal length information is not necessary for the recovery of the tilt but might add more error to the recovery of the slant.

Our experimental results on perceived tilt strongly agrees with above prediction. The data analysis cannot find any effect of viewpoint distortion on tilt perception in terms of tilt sign or absolute tilt error. Our experiment confirms that the large FOV (45^o) cancel the ambiguity in the tilt sign. The viewpoint distortion does not change this effect even when, due to viewpoint distortion, the actual FOV of human subjects is small (15.5^o when viewing distance is 1.2m). Similarly, the absolute tilt error and the effect of the winding angle are not changed under viewpoint distortion. The absolute tilt error increases with the winding angle under all viewpoint distances and projection point distances.

Our experiments on slant show that slant perception is also not significantly affected by viewpoint distortion. We expected that slant perception, which is not reliable even with no viewpoint distortion, will be distorted more because of the viewpoint distortion. However, in our experimental results, we could only observe the further distortion of perceived slant in the case of large slant magnitudes. In the chapter on Computational Interpretation, using the iso-distortion framework, we are able to explain why slant perception, due to a combine effect of errors in various estimates, is not affected significantly by viewpoint distortion. Using the iso-distortion framework, we could also prove that the depth order is preserved, that is, tilt estimation was not significantly affected by the viewpoint distortion.

In conclusion, our experiments showed that human subjects are not significantly af-

fected by the viewpoint distortion in structure from motion. In the literature, in the case of static object, it is reported that the perception of observer is not significantly affected by distortion arising from viewpoint change. Our experiments in structure from motion also report similar results in the case of moving object. Our results can apply for viewers in cinema: their perception of plane orientation in a sequence of moving images will not be significantly affected by their distances to the screen if their seats are near the axis of the projector. Furthermore, from our result, when we design a HMD device for applications in which users need to recover plane orientation from motion, it is acceptable to ignore the viewpoint distortion under the same conditions as our experiment.

7.2 Future work

In our experiments, we have only examined the perception of planar orientation from motion. Besides, the distortion viewpoint investigated is equivalent to a change in the focal length only when the optical axis of subjects are coincident with the optical axis of the projector system. Our experimental motion is also a special one: rotation in depth. Therefore, there are various different conditions that can be further examined on how human being perceives the pictures under viewpoint distortion:

- surface is curved,
- viewpoint is not on the projection axis, and
- different motion, such as motion in depth, pure translation ...

These are the open questions to be investigated to further our understanding on how human perceives the scene using motion cues under viewpoint distortion.

Bibliography

[1] Adiv, G. "Inherent Ambiguities in Recovering 3-D Motion and Structure from a Noisy Flow Field", *IEEE Transactions on Pattern Analysis and Machine Intelligence*, 11(5), 477-489 (1989).

[2] Barrow, H.G. and J.M. Tenenbaum. "Interpreting line drawings as three-dimensional surfaces", *Artificial Intelligence*, 17, 75-116 (1981).

[3] Braunstein, M. L. "Motion and texture as sources of slant information", *Journal of Experimental Psychology*, 78, 247253 (1968).

[4] M. J. Brooks, W. Chojnacki and L. Baumela. "Determining the egomotion of an uncalibrated camera from instantaneous optical flow", *Journal of the Optical Society of America A*, 14(10):2670–2677, 1997.

[5] M. J. Brooks, W. Chojnacki, A. V. D. Hengel and L. Baumela. "Robust techniques for the estimation of structure from motion in the uncalibrated Case". In *Proc. European Conf. on Computer Vision*, pages 283–295,1998.

[6] L-F. Cheong, C. Fermüller, and Y. Aloimonos, "Effects of errors in the viewing geometry on shape estimation", *Computer Vision and Image Understanding*, 71(3):356–372, 1998.

[7] L-F. Cheong and K. Ng, "Geometry of distorted visual space and cremona transformation", *International Journal of Computer Vision*, 32(2):195–212, 1999.

[8] L-F. Cheong and C. H. Peh. "Characterizing depth distortion due to calibration uncertainty", In *Proc. European Conf. on Computer Vision*, pages 664–677, 2000.

[9] L-F. Cheong and T. Xiang. "Characterizing depth distortion under different generic motions", *International Journal of Computer Vision*, 44(3):199–217, 2001.

[10] V. Cornilleau-Pèrés and J. Droulez. "Visual perception of surface curvature: Psychophysics of curvature detection induced by motion parallax", *Perception and Psychophysics*, 46(4):351–364, 1989.

[11] J. Droulez and V. Cornilleau-Pèrés. "Visual perception of surface curvature: the spin variation and its physiological implications", *Biological Cybernetics*, 62:211-224, 1990.

[12] Cornilleau-Prs, V. and J. Droulez. "The visual perception of three-dimensional shape from self-motion and object-motion", *Vision Research*, 34(18), 2331-2336 (1994).

[13] Cornilleau-Prs, V., T.K. Wong, L.F. Cheong and J. Droulez. "Visual perception of slant from optic flow under orthographic and perspective projection", *Invest. Ophthalm. Vis. Sci.*, 41(4), 3820 (2000).

[14] V. Cornilleau-Pèrés, M. Wexler, J. Droulez, E. Marin, C. Miège and B. Bourdoncle. "Visual perception of planar orientation: dominance of static depth cues over motion cues", *Vision Research*, 42, 14031412 (2002).

[15] Dijkstra, T.M.H., V. Cornilleau-Prs, C.C.A.M. Gielen and J. Droulez. "Perception of 3D shape from ego- and object-motion: comparison between small and large filed stimuli", *Vision Research*, 35(4), 453-462 (1995).

[16] Domini, F. and C. Caudek. "Perceiving Surface Slant from Deformation of Optic Flow", *Journal of Experimental Psychology: Human Perception and Performance*, 25, 426-444 (1999).

[17] Domini, F., C. Caudek and S. Richmann. "Distortions of Depth-order Relations and Parallelism in Structure from Motion", *Perception and Psychophysics*, 60, 1164-1174 (1998).

[18] E. Grossmann and J. S. Victor. "Uncertainty analysis of 3D reconstruction from uncalibrated views", *Image Vision Computing*, 18(9):686–696, 2000.

[19] Hagen, M.A."Influence of picture surface and station point on the ability to compensate for oblique view in pictorial perception", Development Psychology, 12(1):57–63 (1976)

[20] R. I. Hartley. "An algorithm for self calibration from several views", In *Proc. IEEE Conf. Computer Vision and Pattern Recognition*, pages 908–912, 1994.

[21] Hoffman, D.D. "Inferring Local Surface Orientation from Motion Fields",*Journal of the Optical Society of America*, 72(7), 888-892 (1982).

[22] B. K. P. Horn. "Motion fields are hardly ever ambiguous", *International Journal of Computer Vision*, 1:259–274, 1987.

[23] B. K. P. Horn and E. J. Weldon. "Computational efficient methods for recovering translational motion", In *Proc. International Conference on Computer Vision*, pages 2–11, 1987.

[24] B. K. P. Horn. Relative orientation. *International Journal of Computer Vision*, 4:59–78, 1990.

[25] F. Kahl. "Critical motions and ambiguous Euclidean reconstructions in auto-calibration", In *Proc. Int. Conf. on Computer Vision*, pages 469–475, 1995.

[26] J. J. Koenderink and A. J. van Doorn. "Invariant properties of the motion parallax field due to the movement of rigid bodies relative to an observer", *Optica Acta*, 22(9):773–791, 1975.

[27] J. J. Koenderink and A. J. van Doorn. "Affine structure from motion", *J. Optic. Soc. Am.*, 8(2):377–385, 1991.

[28] J. J. Koenderink and A. J. van Doorn. "Surface shape and curvature scales", *Image and Vision Computing*, 10(8):557–564, 1992.

[29] J. J. Koenderink and A. J. van Doorn. "Relief: pictorial and otherwise", *Image and Vision Computing,*, 13(5):321–334, 1995.

[30] J. J. Koenderink, A. J. van Doorn, C. Christou and J. S. Lappsin. "Shape constancy in pictorial relief", In *Object Representation in Computer Vision II. European Conf. on Computer Vision International Workshop*, pages 151–164, 1996.

[31] H. C. Longuet-Higgins. "A computer algorithm for reconstruction of a scene from two projections", *Nature* , 293:133-135, 1981.

[32] H. C. Longuet-Higgins. "The visual ambiguity of a moving plane", *Proc. R. Soc. Lond.* , B233:165-175, 1984.

[33] S. J. Maybank and O. D. Faugeras. "A theory of self-calibration of a moving camera",*International Journal of Computer Vision*, 8(2):123–151, 1992.

[34] Rosinki,R.R., Mulholland, T., Degelman,D., and Farber, J., "Picture perception: An analysis of visual compensation", *Perception and Psychophysics*, 28(6): 521–526 (1980).

[35] M. Pollefeys, R. Koch and L. Gool. "Self-calibration and metric reconstruction in spite of varying and unknow internal camera parameters" ,In *Proc. Int. Conf. on Computer Vision*, pages 90–95, 1998.

[36] K. Prazdny. "Egomotion and relative depth map from optical flow", *Biological Cybernetics*, 36:87-102, 1980.

[37] P. Sturm. "Critical motion sequences for monocular self-calibration and uncalibrated Euclidean reconstruction", In *Proc. Conf. Computer Vision and Pattern Recognition*, pages 1100–1105, 1997.

[38] J. T. Todd and F.D. Reichel. "Ordinal structure in the visual perception and cognition of smoothly curved surfaces", *Psychological Review*, 96(4):643–657, 1989.

[39] S. Ullman, *The Interpretation of Visual Motion*. MIT Press, Cambridge and London, 1979.

[40] A. Verri and E. Trucco. "Finding the epipole from uncalibrated optical flow", In *Proc. Int. Conf. on Computer Vision*, pages 987–991, 1998.

[41] T. Viéville and O. D. Faugeras. "The first-order expansion of motion equations in the uncalibrated case", *Computer Vision and Image Understanding*, 64(1):128–146, 1995.

[42] T. Xiang and L-F. Cheong. "Understanding the behavior of structure from motion algorithms: a geometric approach". *International Journal of Computer Vision*, 51(2), 111137, 2003.

[43] Lee, D.N., "The optical flow field: the foundation of vision", *Phil. Trans. R. Soc. London Ser. B*, 290, 169-179 (1980).

[44] D. N. Perkins, "Compensating for distortion in viewing pictures obliquely",*Perception and Psychophysics*, 14:13–18, (1973).

[45] Rogers, B., and M. Graham. "Motion Parallax as an Independent Cue for Depth Perception", *Perception*, 8, 125-134 (1979).

[46] Stevens, K. A., "Surface tilt (the direction of slant): a neglected psychophysical variable", *Perception and Psychophysics*, 33, 241250 (1983).

[47] Subbarao, M. "Interpretation of Visual Motion: A computational study", Morgan Kaufmann Publishers (1988).

[48] Todd, J. T. and P. Bressan. "The perception of 3-dimensional affine structure from minimal apparent motion sequences", *Perception and Psychophysics*, 48(5), 419-430 (1990).

[49] Todd, J.T. and V.J. Perotti. "The visual perception of surface orientation from optical flow", *Perception and Psychophysics*, 61(8), 1577-1589 (1999).

[50] Yeow, M.G. "The perception of slant from motion in large-field vision", M.Eng thesis, National University of Singapore (2000).

[51] Zhong, H., V. Cornilleau-Prs, L.F. Cheong and J. Droulez. "The visual perception of plane tilt from motion in small field and large field: Psychophysics and theory", *Vision Research* 46, pages 34943513(2006).